Table EA-1. Stream-water dissolved Mn at basin outflow of perennial stream at Inspiration Dam illustrating decreases in dissolved Mn in response to remediation efforts. Dissolved Mn in moles/L. Sampling and analysis methods described in Harvey and Fuller (1998).

Date	Mn (moles/L)	
22-May-97	5.0E-04	R2B sampled
24-Jul-97	4.9E-04	
25-Sep-97	5.1E-04	
22-Jan-98	3.0E-04	
24-Mar-98	3.6E-04	
01-Jun-98	1.5E-04	Z9A sampled
27-Jul-98	2.8E-04	
24-Nov-98	3.6E-04	
11-Feb-99	1.2E-05	Remedial ground-water pumping begins
24-Mar-99	8.9E-06	
23-Apr-99	1.1E-05	
15-Jun-99	1.8E-05	
24-Aug-99	7.1E-05	
19-Oct-99	9.1E-05	
17-Dec-99	4.0E-05	
29-Dec-99	3.0E-05	Discharge of treated water to stream channel begins
15-Feb-00	2.7E-05	AK1 sample
13-Apr-00	1.3E-05	
18-Apr-00	4.0E-06	
13-Jun-00	6.7E-06	
20-Jul-00	4.9E-06	
15-Dec-00	1.4E-05	
07-Feb-01	4.0E-06	
11-Jun-01	4.2E-06	SIQ deployment
24-Oct-01	6.8E-06	
15-Jan-02	3.3E-06	

Table EA-2. Stream water (SW) and ground-water (GW) chemistry data for streambed sediment sampling sites. Dissolved concentrations in mole/L. Samples were collected within two days of sediment sampling. Sampling and analysis methods are described in Fuller and Harvey (2000).

Site	R2B	R2B	Z9A	Z9A	AK1
	SW	GW	SW	GW	SW
pH	6.9	6.6	7.0	6.4	6.7
Mn	8.2E-04	3.2E-04	7.3E-04	8.2E-05	1.7E-04
Co	3.6E-06	<3E-07	2.7E-06	<3E-07	<2E-07
Ni	8.0E-06	<1.5E-06	8.5E-06	<1.5E-06	<3E-07
Zn	5.9E-06	<3E-07	5.8E-06	<3E-07	<5E-07
Al	6.0E-06	<4E-06	5.2E-06	<4E-06	<5E-07
Cu	<2E-07	<5E-07	<2E-07	<5E-07	<2E-07
Fe	<2E-07	<5E-07	<5E-07	<5E-07	<5E-07
Ca	9.8E-03	1.0E-02	9.7E-03	9.7E-03	1.0E-02
Si	1.0E-03	8.4E-04	2.2E-03	1.8E-03	1.0E-03
K	1.9E-04	1.2E-04	2.3E-04	1.8E-04	1.5E-04
Mg	3.8E-03	3.8E-03	3.8E-03	3.5E-03	2.2E-03
Na	2.5E-03	2.5E-03	2.8E-03	2.7E-03	2.9E-03
Sr	1.6E-05	1.7E-05	1.6E-05	1.7E-05	1.4E-05
SO_4	1.4E-02	1.3E-02	1.4E-02	1.2E-02	1.5E-02
Cl	1.3E-03	1.1E-03	1.4E-03	1.2E-03	1.3E-03
Alkalinity	4.8E-04	1.5E-03	4.4E-04	1.4E-03	4.2E-04

Figure EA-1. Pinal Creek study area map showing location of streambed sampling sites.

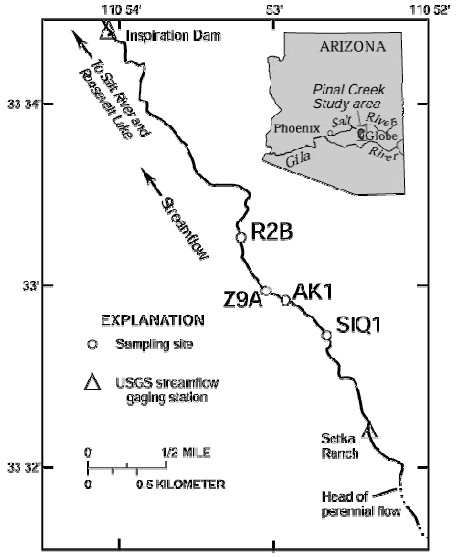

Figure EA-2. Area XRD diffraction pattern from grain R2B2-01. D-spacings are noted at right margin.

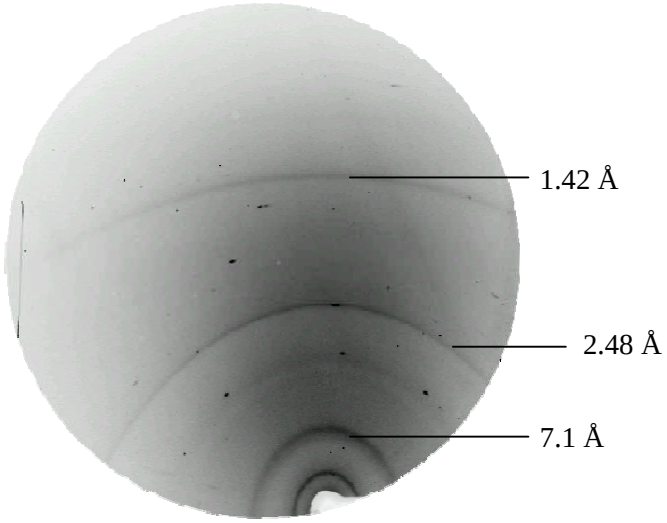

Figure EA-3. Normalized XANES spectra (solid lines) from Pinal Creek samples. Spectrum HB is from hexagonal birnessite. Other sample labels correspond to labels in Table 2. Approximate positions of absorbance maxima for Mn(II) (from $MnCl_2$) and Mn(IV) (hexagonal birnessite) are indicated with vertical lines. Fits are represented by dotted lines.

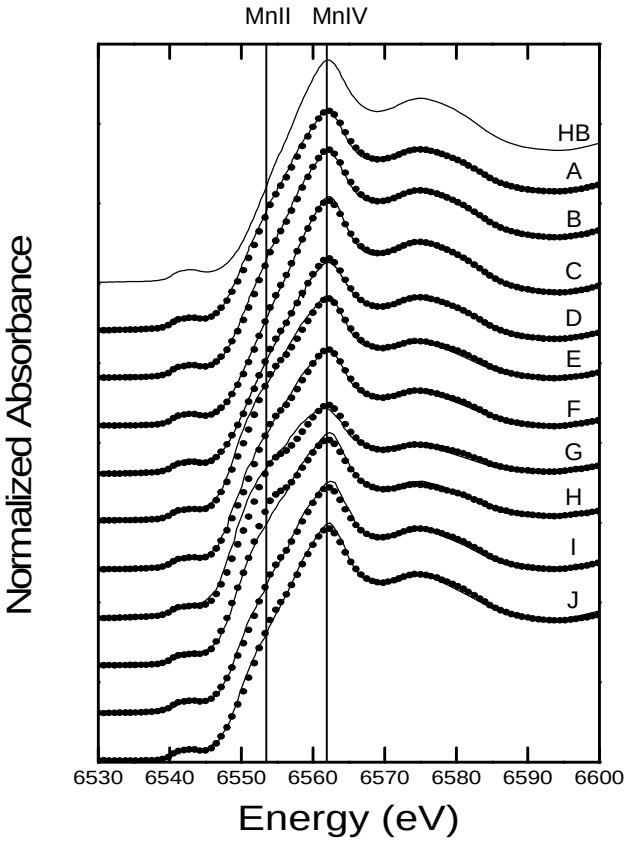

Figure EA-4. Mn-O shell FT peak height compared to EXAFS fit-derived Mn-O shell splitting for samples E-J (individual grain coating micro-locations). Bulk EXAFS data have 2.5-fold less Mn(II), which offsets the data points as compared to the micro-EXAFS data, and hence can not be compared on the same plot.

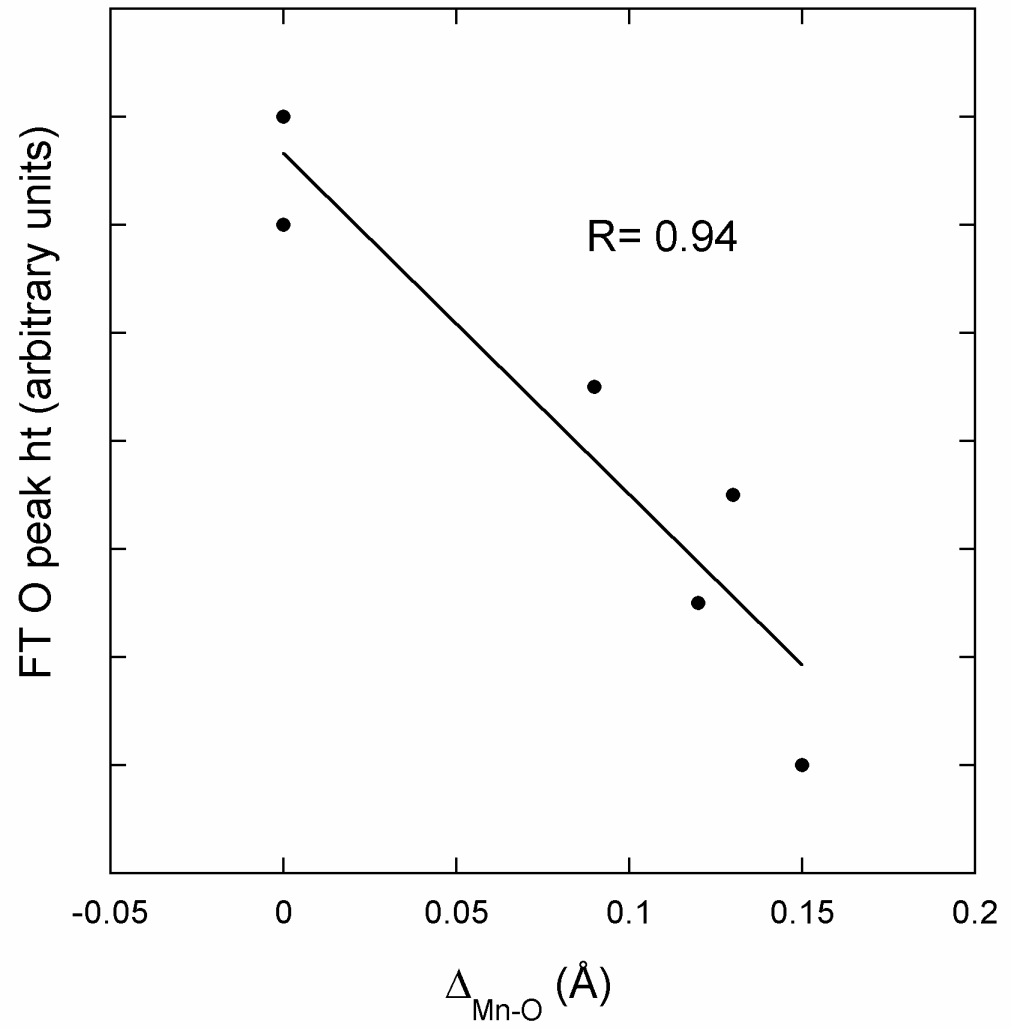

Description of particle size estimation based on powder diffraction data

To estimate the effective diameters of the Mn oxide particles, simulations of experimentally observed Scherrer rings were performed to quantify the root-mean-square (rms) intensity variation of the ring as a function of particle size. Five major steps were performed in this process. (i) In a mathematical simulation, diffracting rays were randomly projected to positions around the 2.48 Å Scherrer ring (*i.e.*, around the Eulerian angle, ?). The width of each simulated diffracted ray was estimated as follows: the width along the 2-theta direction was taken to be equivalent to the experimental data. The width for the peak in the ? direction (*i.e.*, along the Scherrer ring) is expected to be somewhat larger than along the 2-theta direction because the reciprocal lattice points for 2-D particles are in fact rods in reciprocal space, with the long axis corresponding to the out-of-plane direction. The length:width aspect ratio of the reciprocal lattice rods is estimated to be ~ 4, based on coherent scattering domain (CSD) dimensions of 2 nm normal to the layers, and 8.5 nm for the in-plane direction, reported for biogenic Mn oxides produced by *P. putida* (Villalobos *et al.*, 2006). About half of the reflections have these rods oriented tangential to the Ewald sphere (AZAROFF, 1968) during diffraction. The peak width in the direction around ? was subsequently assumed to be twice as large as in the direction along the 2-theta. It was found that 2.5×10^5 diffracting rays were required to reproduce the observed rms intensity variation of 1.4% along the Scherrer ring. The error in the above-described peak width estimate is bounded by a factor of two. The uncertainty corresponding to one estimated standard deviation was subsequently estimated to be half of the maximum uncertainty, *i.e.*, 1s = 25%. (ii) The number of diffracted rays was scaled to reflect the fact that only a small fraction of the grains in a randomly oriented powder will be aligned to diffract into the 2.48 Å Scherrer ring. The fraction of particles that could satisfy diffraction condition was taken to be equivalent to the full-width-half-max area of the Scherrer ring on the Ewald sphere (0.029 $Å^{-2}$ at ? = 1.377 Å) divided by the entire surface area of the Ewald sphere (6.626 $Å^{-2}$), *i.e.*, 0.38% ± .019%. (iii) The number of particles was scaled to reflect the 6-fold

redundancy of diffraction into the 2.48 Å peak. Taking these corrections into account, it was estimated that *ca* 2.3% of all grains, *i.e.*, $1.1\pm0.29 \times 10^7$ randomly oriented crystalline particles are required to reproduce the observed 1.4% rms intensity variation around ?. (iv) The scattering volume of the sample was scaled to account for the low density open structure of the Mn oxide coatings apparent in SEM images (*vida infra*). Mn K-edge absorption cross-sections of these samples indicate that the effective Mn thickness of the Mn oxides is only about 3 ± 0.15 μm (*i.e.*, 1/10 the 30 μm polished sample thickness). Therefore, the relevant sample volume is estimated to be 10% of the 1,200 μm^3 illuminated volume, or 120 ± 6 μm^3. (v) This scattering volume was divided by 1.1×10^7 scattering to obtain an effective scattering particle volume of $1.09\pm0.29 \times 10^{-5}$ μm^3. Assuming spherical particles, one concludes that each diffracting particle has an effective diameter of *ca* 28 ± 13 nm. More properly, the particles shape can be taken as cylindrical plates of thickness estimated using the Scherrer equation applied to the 10 Å (001) reflection (R2B bulk sample), which results in a thickness estimate of 11.6 ± 0.5 nm. Using this value to estimate lateral sheet dimension, an average particle diameter of 35 ± 13 nm is obtained.

References not cited in the main paper

Azaroff L. V. (1968) *Elements of X-Ray Crystallography*. McGraw-Hill.